2012

The Chloroplast Triggers Developmental Reprogramming When MUTS HOMOLOG1 Is Suppressed in Plants

Ying-Zhi Xu
University of Nebraska - Lincoln, ying-zhi.xu@unl.edu

Roberto de la Rosa Santamaria
Colegio de Postgraduados Campus

Kamaldeep S. Virdi
University of Nebraska-Lincoln

Maria P. Arrieta-Montiel
University of Nebraska-Lincoln

Fareha Razvi
University of Nebraska-Lincoln

See next page for additional authors

The Chloroplast Triggers Developmental Reprogramming When MUTS HOMOLOG1 Is Suppressed in Plants[1][W][OA]

Ying-Zhi Xu, Roberto de la Rosa Santamaria, Kamaldeep S. Virdi, Maria P. Arrieta-Montiel, Fareha Razvi, Shaoqing Li, Guodong Ren, Bin Yu, Danny Alexander, Lining Guo, Xuehui Feng, Ismail M. Dweikat, Tom E. Clemente, and Sally A. Mackenzie*

Center for Plant Science Innovation (Y.-Z.X., R.d.l.R.S., K.S.V., M.P.A.-M., F.R., S.L., G.R., B.Y., X.F., T.E.C., S.A.M.) and Department of Agronomy and Horticulture (R.d.l.R.S., X.F., I.M.D., T.E.C., S.A.M.), University of Nebraska, Lincoln, Nebraska 68588–0660; Colegio de Postgraduados Campus, Tabasco, Mexico 86570 (R.d.l.R.S.); College of Life Sciences, Wuhan University, Wuhan 430072, People's Republic of China (S.L.); and Metabolon, Inc., Durham, North Carolina 27713 (D.A., L.G.)

Multicellular eukaryotes demonstrate nongenetic, heritable phenotypic versatility in their adaptation to environmental changes. This inclusive inheritance is composed of interacting epigenetic, maternal, and environmental factors. Yet-unidentified maternal effects can have a pronounced influence on plant phenotypic adaptation to changing environmental conditions. To explore the control of phenotypy in higher plants, we examined the effect of a single plant nuclear gene on the expression and transmission of phenotypic variability in Arabidopsis (*Arabidopsis thaliana*). MutS HOMOLOG1 (MSH1) is a plant-specific nuclear gene product that functions in both mitochondria and plastids to maintain genome stability. RNA interference suppression of the gene elicits strikingly similar programmed changes in plant growth pattern in six different plant species, changes subsequently heritable independent of the RNA interference transgene. The altered phenotypes reflect multiple pathways that are known to participate in adaptation, including altered phytohormone effects for dwarfed growth and reduced internode elongation, enhanced branching, reduced stomatal density, altered leaf morphology, delayed flowering, and extended juvenility, with conversion to perennial growth pattern in short days. Some of these effects are partially reversed with the application of gibberellic acid. Genetic hemicomplementation experiments show that this phenotypic plasticity derives from changes in chloroplast state. Our results suggest that suppression of *MSH1*, which occurs under several forms of abiotic stress, triggers a plastidial response process that involves nongenetic inheritance.

Plants display a surprising capacity for rapid adaptation. The phenotypic response to environmental change is thought to include nongenetic, transgenerational processes (Bonduriansky and Day, 2009) that likely integrate epigenetic and/or maternal factors (Johannes et al., 2008; Danchin et al., 2011). Although maternal effects have been shown to influence these plant responses (Galloway, 2005), the involvement of organellar processes has not been formally demonstrated.

The *MutS HOMOLOG1* (*MSH1*) gene is unique to plants and encodes a homolog to the bacterial mismatch repair protein MutS (Abdelnoor et al., 2003), with at least two important changes within the plant lineage during its evolution. The first involved a C-terminal fusion to a GIY-YIG homing endonuclease domain (VI; Abdelnoor et al., 2006), and the second involved the inclusion of hydrophobic stretches within the region linking essential DNA binding (I) and ATPase (V) domains. These and other sequence features distinguish the plant protein from any other MutS homolog yet identified (Ogata et al., 2011) and presumably confer unique functional properties.

The MSH1 protein is dual targeting, localized to both mitochondrial and chloroplast nucleoids (Xu et al., 2011). Disruption of MSH1 enhances recombination at 47 pairs of repeated sequences in the mitochondrial genome of Arabidopsis (*Arabidopsis thaliana*; Shedge et al., 2007; Arrieta-Montiel et al., 2009; Davila et al., 2011) and gives rise to cytoplasmic male sterility in tomato (*Solanum lycopersicum*) and tobacco (*Nicotiana tabacum*; Sandhu et al., 2007). Within the chloroplast, disruption of *MSH1* results in low-frequency DNA rearrangements mediated by recombination, together with altered redox properties of the cell and variegation of the plant (Xu et al., 2011). In both cytoplasmic male sterility and variegation, the altered phenotype appears to derive from organellar genomic

[1] This work was supported by the National Science Foundation Plant Genome Research Program (grant no. IOS 0820668 to S.A.M.).

* Corresponding author; e-mail smackenzie2@unl.edu.

The author responsible for distribution of materials integral to the findings presented in this article in accordance with the policy described in the Instructions for Authors (www.plantphysiol.org) is: Sally A. Mackenzie (smackenzie2@unl.edu).

[W] The online version of this article contains Web-only data.

[OA] Open Access articles can be viewed online without a subscription.

www.plantphysiol.org/cgi/doi/10.1104/pp.112.196055

rearrangement, displaying subsequent maternal inheritance with incomplete penetrance.

Here, we have carried out cross-species comparative studies of *MSH1* suppression to investigate phenotypic changes that occur in response to organellar perturbation but do not appear attributable to organellar genome instability. These studies produced evidence of developmental reprogramming in response to chloroplast signals that accompany MSH1 suppression. Remarkably, these developmental changes, once effected, are stable, heritable, and independent of the RNA interference (RNAi) transgene in subsequent generations, suggesting that these organellar signals influence epigenetic properties of the plant.

RESULTS

MSH1 Suppression Has Similar Phenotypic Effects in Multiple Plant Species

Whereas *MSH1* was originally identified in Arabidopsis, subsequent studies of its properties were investigated by RNAi suppression of *MSH1* orthologs in other plant species, including the monocots sorghum (*Sorghum bicolor*) and millet (*Pennisetum americanum*) and the dicots soybean (*Glycine max*), tobacco, and tomato. Comparative analysis of MSH1 depletion in these lines produced similar phenotypic changes beyond male sterility and variegation in each species, involving dwarfed growth and reduced internode elongation, enhanced branching, altered leaf morphology, extended juvenility, and delayed flowering, as shown in Figure 1. In tobacco, the most pronounced features of the MSH1-dr growth included a dramatic range of altered leaf morphologies, ranging from extremely large and rounded to very narrow and pointed in shape. Delays in tobacco flowering included plants that never flowered and continued to grow vegetatively. Many plants showed extensive alteration in branching pattern (Fig. 1). In soybean, leaf morphology was the most pronounced effect in the dwarfed plants, with leaf wrinkling that resembled virus infection. These plants also showed dramatic delays in flowering.

In sorghum, where phenotypic variation was analyzed in detail, *MSH1* suppression produced dramatic changes in plant tillering, height, internode elongation, and stomatal density (Supplemental Fig. S1; Supplemental Table S2). These phenotypic changes were characterized as developmental reprogramming (MSH1-dr), given their cross-species reproducibility and influence on numerous aspects of development.

Phenotypic sorting allowed the discrimination of independently sorting and separable developmental changes: variegation, male sterility, and the dwarfed/tillered/delayed-flowering phenotypes. The dwarf phenotype was consistently coinherited with enhanced tillering/altered branching and flowering delay in all plant species, with the phenotype appearing in approximately 20% of the original, unselected *msh1* population in Arabidopsis. The phenotype appeared in about 40% of the T3 families in sorghum, at an average frequency of 20% in those families in which it was observed (Supplemental Table S1). Because our initial focus for these studies was on documenting the male-sterility phenotype, we did not characterize the exact frequency of the MSH1-dr phenotype in early generations; our detailed characterization of the phenotype was initiated in the T3 generation.

In the Arabidopsis *msh1* mutant, plants showed a range in the severity of the altered phenotype, with approximately 20% clearly dwarfed and 100% delayed in flowering. Selection for the dwarfed plants effectively shifted the resulting population to an approximately 80% dwarfed, delayed-flowering type (Fig. 2A; Table I) that, under 10-h daylength, displayed perennial growth features, including aerial rosettes, dramatic elongation of lifespan, and enhanced secondary growth of the stem (Fig. 2). This delay in flowering was associated with a delay in maturity transition, evident in leaf shape (Fig. 2F). The dwarf *msh1* mutant

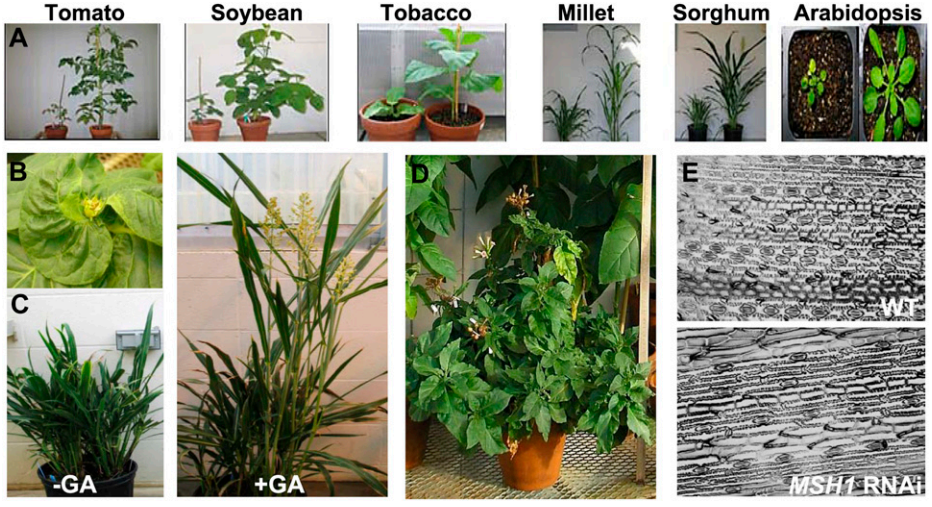

Figure 1. Loss of *MSH1* results in programmed phenotypic changes. A, A dwarf phenotype is evident in six plant species with RNAi suppression or mutation (Arabidopsis) of *MSH1*. B, Altered leaf morphology in an *MSH1*-RNAi tobacco line. C, Evidence of phenotype reversibility in sorghum with application of 2,500 ppm GA. D, Enhanced branching phenotype in an *MSH1*-RNAi line of tobacco. E, Reduced stomatal density on the leaf surface of *MSH1*-RNAi sorghum.

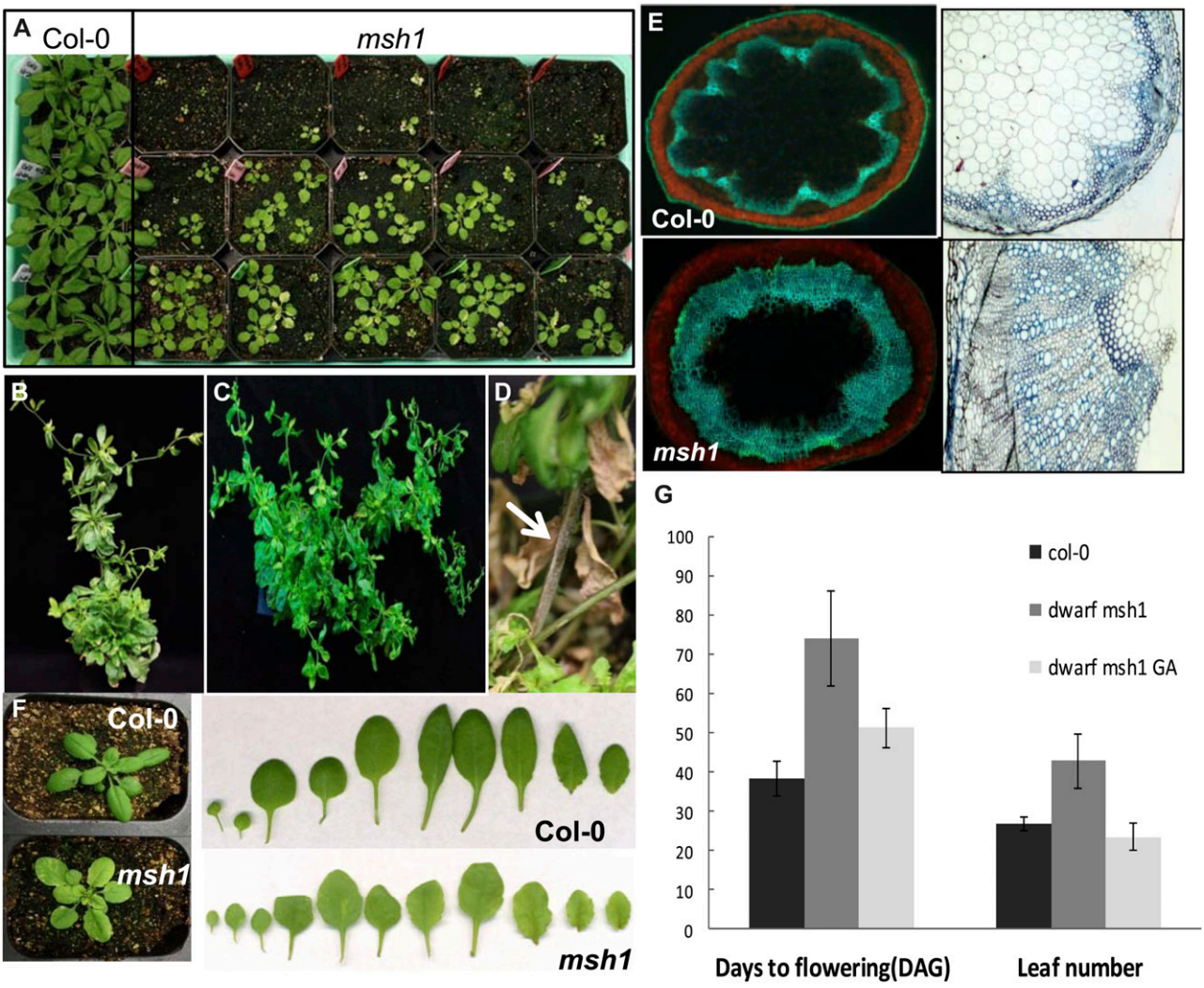

Figure 2. Phenotypic plasticity in the Arabidopsis *msh1* mutant. A, The *msh1* mutant, grown under a 12-h daylength, is dwarfed and the frequency of the dwarf delayed-flowering phenotype increases with selection. B and C, Under a 10-h daylength, vegetative growth in the *msh1* mutant is markedly extended, with plants displaying aerial rosettes (B) and extensive branching (C). These plants are 4 to 5 months old. D and E, The *msh1* plants also display thickened stems (D) and secondary growth (E). Autofluorescence in stem cross-sections from the *msh1* mutant and the Col-0 wild type shows plastids (red) in the cortex and lignin (blue-green) in the xylem. Light microscopy of toluidine blue-stained sections shows extensive secondary xylem in the mutant relative to the wild type (200×). F, Three-week-old Col-0 and *msh1* plants grown in a 12-h daylength and showing evidence of a prolonged juvenile phase in the *msh1* mutant. G, Dwarf *msh1* plants show flowering time response to treatment with 100 mM GA twice per week. Arabidopsis flowering time was recorded as the date of first visible flower bud appearance (DAG, days after germination). At this time, total rosette leaf number was also recorded. Data shown are means ± SE from 10 plants.

phenotype in Arabidopsis showed partial reversal with GA application (Fig. 2G; Table II).

The Altered Growth Patterns Are Retained after Segregation of the RNAi Transgene

In sorghum, individuals displaying the MSH1-dr phenotype gave rise to progeny populations fully penetrant for the phenotype (100% dwarfed/enhanced tillering/delayed flowering). Upon segregation of the RNAi transgene in a hemizygous plant displaying the MSH1-dr phenotype, the phenotype was again fully penetrant in the progeny population, regardless of transgene segregation. These observations permitted the development of sorghum lines, devoid of the RNAi transgene, that bred true for the MSH1-dr phenotype over multiple cycles of self-pollination, with six generations confirmed to date (Table III). The altered phenotype could also be partially reversed by spraying the leaves with 2,250 ppm GA_3 (Fig. 1C).

Although genetic segregation for the RNAi transgene did not reverse the altered dwarf phenotype in sorghum, nontransgenic segregants displayed slight

Table I. *Arabidopsis changes in growth with loss of MSH1*

Line	No. of Plants	Diameter	Days to Flower	Rosette Leaf No.
		cm		
Col-0	22	17.9 ± 1.1	38.2 ± 4.4	26.9 ± 1.7
msh1[a]	17	7.1 ± 2.7	74.0 ± 12	42.9 ± 6.9

[a]*msh1* mutants were selected for the dwarf phenotype.

changes in flowering. Transgenic plants were nonflowering unless treated with GA; nontransgenic plants were delayed in flowering but did not require GA treatment. In nontransgenic plants, *MSH1* transcript levels and *MSH1* DNA methylation pattern reverted to wild-type levels (Fig. 3; Supplemental Fig. S3). These results imply that heritability and transgenerational stability of the altered phenotypes were not likely consequences of the RNAi-induced stable silencing of the *MSH1* locus. Reciprocal crossing of the dwarf sorghum lines, lacking transgene, to the wild type (inbred Tx430) resulted in complete reversal of the dwarf and delayed-flowering phenotype in the F1 progeny (Fig. 4; Supplemental Table S3). Thus, *MSH1* modulation appears to condition changes within the plant that are heritable through self-pollination but reversed through crossing to the wild type. Identical reciprocal crossing results showing reversal of phenotypes imply that these heritable changes are not organellar. In the subsequent F2 generation, we also observed no evidence of the dwarf phenotype, as would be expected if the trait were conditioned by a single recessive locus that was segregating (data not shown).

MSH1 Suppression Alters Numerous Plant Pathways

Transcript profiling and reverse transcription (RT)-PCR experiments in the Arabidopsis *msh1* mutant identified several nuclear gene expression changes underlying the altered growth types (Table IV). Pathways associated with dwarfing include cell cycle regulation and increased GA catabolism (Tables II and IV; Fig. 5A). Alterations in leaf morphology and branching are likely consequences of changes in auxin production and receptor expression (Willige et al., 2011). Effects on flowering and conversion to a perennial growth pattern were associated with changes in the expression of flowering and vernalization regulators (Fornara et al., 2010), including increased *FLOWERING LOCUS C SUPPRESSOR OF OVEREXPRESSION OF CO1* (*FLC*) and decreased *SUPPRESSOR OF OVEREXPRESSION OF CO1* (*SOC1*) expression (Fig. 5B), as well as increased *miR156* and decreased *miR172* levels (Fig. 5C).

Disruption of *MSH1* has a similarly marked influence on stress response pathways. Both transcript and metabolic profiling experiments revealed organelle-influenced metabolic changes underlying the variability in plant growth and reflective of plant responses to stress conditions (Tables IV and V). Metabolic changes in the sorghum dwarf plants were concentrated within TCA flux. Increased energy metabolism in the dwarf line reflected the up-regulation of most compounds of the TCA, NAD, and carbohydrate metabolic pathways and the down-regulation of amino acid biosynthesis, reflecting altered carbon/nitrogen balance in these plants. In Arabidopsis, this alteration was most evident in the depletion of Suc to undetectable levels. Metabolic priming for environmental stress in sorghum may be evident in the 1.2- to 5.7-fold elevation of sugar and sugar alcohol levels, an effect that stabilizes osmotic pressure in response to stresses like drought (Ingram and Bartels, 1996). The antioxidants ascorbate and α-tocopherols were increased, together with the stress-responsive flavones apigenin, apigenin-7-*O*-glucoside, isovitexin, kaempferol 3-*O*-β-glucoside, luteolin-7-*O*-glucoside, and vitexin. In Arabidopsis, the response included an increase in oxidized glutathione as well as sinapate, likely signaling induction of the phenylpropanoid pathway, together with the polyamines 1,3-diaminopropane, putrescine, and spermidine, which likely influence both stress tolerance and the observed delay in maturity transition (Gill and Tuteja, 2010).

The Observed Developmental Reprogramming Is the Consequence of Chloroplast Changes

Although several identifiable and intersecting nuclear gene expression networks are altered in the phenotypic variants, MSH1 is an organellar protein. We used genetic hemicomplementation to discriminate between mitochondrial and plastidial influences on *msh1*-associated phenotypy. Hemicomplementation lines were developed in Arabidopsis by transgenic introduction of a mitochondria- versus plastid-targeted form of *MSH1* to a *msh1* mutant as described previously (Xu et al., 2011). Transgenic lines containing the plastid-targeted form of MSH1 undergo mitochondrial DNA recombination (Xu et al., 2011) but show no evidence of reduced growth rate, delayed flowering, or altered leaf morphology (Figs. 6 and 7). Lines containing the mitochondria-targeted form of *MSH1* contain a stable mitochondrial genome and produce leaf variegation (Xu et al., 2011) but also display dwarfing, changes in leaf morphology and flowering time, and delayed transition to maturity and senescence (Figs. 6 and 7). These

Table II. *Changes in GA content with loss of MSH1*[a]

N.D., The metabolite was undetectable.

GA	Sorghum		Arabidopsis	
	Tx430	*MSH1*-RNAi	Col-0	*msh1*
GA53	54 ± 12	24 ± 4	7 ± 0	N.D.
GA19	168 ± 7	125 ± 4	11 ± 0	N.D.
GA44	24 ± 7	N.D.		

[a]Sorghum and Arabidopsis lines selected for testing showed the dwarf phenotype. Sorghum lines were positive for the transgene.

Table III. *Inheritance of the dwarf phenotype in T3, T4, and T5 generations after initial selection of the MSH1-dr (dwarf, high tillering, delayed flowering, nontransgenic) lines in T2*

After selection for the MSH1-dr phenotype, all plants showed the dwarf trait in each generation, and these also showed enhanced tillering and delayed flowering, so plant height was used as the measure. Although only three generations are shown, stable heritability of the phenotype has been observed over six generations. All T3, T4, and T5 plants were significantly lower in plant height than the wild-type Tx430 ($P < 0.001$). Lack of the *MSH1*-RNAi transgene was confirmed in all populations by PCR (Supplemental Fig. S2). The first two characters of each line designate the generation, and the remainder is an in-laboratory designator for the family.

Lines	No.	Plant Height	SE
		mean cm	
TX430	30	97.6	3.7
MSH1-dr			
T3GAII	17	52.4	2.7
T4GAII3	18	43.7	4.3
T4GAII5	18	41.4	5.2
T4GAII6	18	40.5	4.9
T4GAII11	17	59.6	4.5
T4GAII15	19	45.1	5.6
T4GAII22	18	56.1	4.4
T4GAII23	15	55.1	4.6
T4GAII24	17	45.8	4.7
T4GAII25	15	44.0	4.6
T4GAII27	16	52.9	5.5
T4GAII28	18	56.5	4.1
T5GAII3	5	47.0	2.8
T5GAII5	5	43.6	2.3
T5GAII6	5	45.4	3.2
T5GAII11	5	40.8	3.0
T5GAII15	5	45.4	1.5
T5GAII22	5	52.2	5.0
T5GAII23	5	53.2	3.2
T5GAII24	5	53.4	3.2
T5GAII25	5	51.0	4.3
T5GAII27	5	46.8	4.4
T5GAII28	5	52.4	0.5

observations, supporting plastidial influence on phenotype, were supported by metabolic profiles from the hemicomplementation lines. Metabolic profiling of the mitochondria- versus plastid-complemented lines showed very little metabolic difference between the wild type and the chloroplast-complemented lines but produced an array of metabolic changes conditioned by MSH1-deficient chloroplasts in the mitochondria-complemented lines (Fig. 5D). In Arabidopsis, where advanced-generation *msh1* mutants show evidence of mitochondrial DNA changes (Davila et al., 2011), chloroplast DNA rearrangements in Arabidopsis *msh1* are extremely low in frequency and restricted to the variegated sectors (Xu et al., 2011). Analysis of mitochondrial and chloroplast DNA in transgene-minus sorghum lines by similar Illumina deep-sequence-based analysis to that used in Arabidopsis has revealed no evidence of DNA changes to date (Xu et al., 2011; data not shown). To our knowledge, no previously reported chloroplast genome mutation has been shown to produce plant developmental changes similar to those we report here. These considerations, together with the demonstrated reversal of phenotype in sorghum lines crossed to the wild type, provide little or no support for organellar DNA rearrangement underlying the altered growth phenotypes. We postulate that the observed gene expression changes observed in the Arabidopsis dwarf,

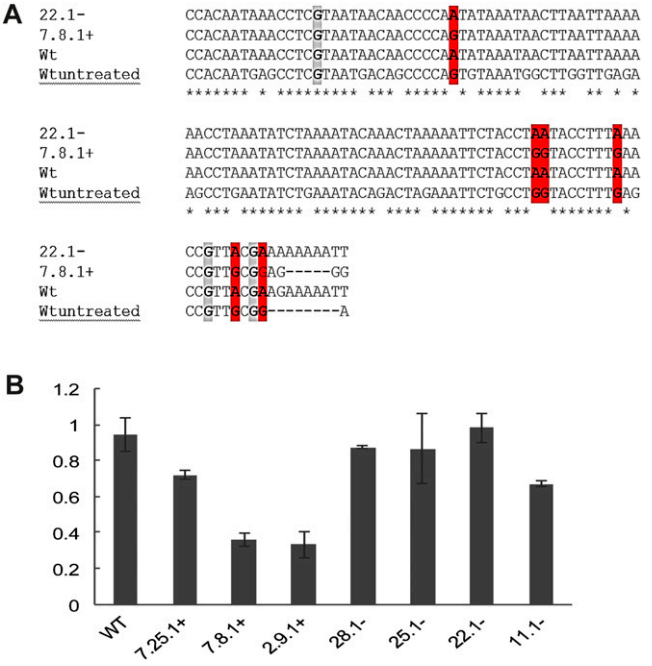

Figure 3. *MSH1* methylation and gene expression. A, Sample bisulfite sequencing of the RNAi-targeted region of *MSH1* in dwarf sorghum plants. Total genomic DNA from T4 dwarf plants with (DW7.8.1) and without (GAII22.1) the *MSH1*-RNAi transgene, and from wild-type Tx430, was bisulfite treated, PCR amplified, and DNA sequenced. The sequence alignment shows results from wild-type Tx430 untreated DNA (Wtuntreated), wild-type Tx430 bisulfite-treated DNA (Wt), the dwarfed line minus transgene (22.1−) bisulfite-treated DNA, and the dwarfed line plus transgene (7.8.1+) bisulfite-treated DNA. Sample data for additional plants tested are shown in Supplemental Figure S3. Red boxes designate points at which cytosines were methylated in the presence of the RNAi transgene but reverted to nonmethylated when the transgene was lost. Gray boxes designate points where methylation was present in the wild type and unaffected by the transgene. The sequence interval shown is that targeted by the RNAi transgene and contained within domain VI of *MSH1*. B, Quantitative RT-PCR analysis of *MSH1* transcript levels in variant-phenotype sorghum plants with (+) and without (−) the *MSH1*-RNAi transgene relative to wild-type Tx430 (WT). Data from 1-week-old seedlings from three T4 lines containing the transgene (7.25.1+, 7.8.1+, 2.9.1+) and four T4 lines minus the transgene (GA28.1−, GA25.1−, GA22.1−, GA11.1−) are shown relative to the wild-type inbred Tx430. The results are from three independent experiments. Some variation in transcript levels is evident, so that line 7.25.1+ shows elevated levels of *MSH1* transcript relative to the other transgenic selections. This line is hemizygous for the transgene, whereas the other two lines are homozygous. The lines tested are T4 generation plants, where we have shown that the phenotype is stable with or without the transgene. As a consequence, we assume that this elevated level of *MSH1* segregating within the T4 generation does not noticeably influence phenotype.

Figure 4. Reversal of the *MSH1*-RNAi phenotype by crossing in sorghum. The *MSH1*-RNAi-altered phenotype in sorghum is characterized by dwarfed growth, enhanced tillering, altered leaf morphology, delayed flowering, and reduced stomatal density. The plant shown at left no longer contains the RNAi transgene. The F1 plant was derived by crossing a sorghum *MSH1*-RNAi-derived line, displaying the altered phenotype but minus the transgene, with the wild-type Tx430 inbred as pollen parent. Both lines shown were derived from Tx430.

delayed flowering lines are conditioned by a change in organellar signal after *MSH1* suppression, not by stable organelle genome rearrangement.

DISCUSSION

The results we present, suggesting chloroplast influence on multiple growth parameters, are not entirely surprising; GA biosynthesis, light response, and vernalization pathways involve chloroplast processes. Mutation of the *CND41* gene in tobacco, encoding a chloroplast nucleoid protein with protease activity, can result in the reduction of GA_1 levels and a dwarf phenotype (Nakano et al., 2003). Disruption of *HSP90* genes, some of which encode organellar products, has been associated with dramatic changes in plant development, including altered chloroplast development (Sangster and Queitsch, 2005). However, *HSP90*-associated phenotypic changes do not appear to resemble the processes we describe here, and *HSP90* expression is unchanged in the *msh1* mutant.

What is surprising in *MSH1* depletion is not simply the array of phenotypes that emerge but the programmed and heritable manner in which these intersecting nuclear gene networks respond to organelle perturbation. Numerous genetic mutations are shown to alter chloroplast functions, many producing variegation phenotypes (Sakamoto, 2003; Yu et al., 2007). Yet, no association has been reported of these mutations with similar, developmental reprogramming, implying that a specificity of function rather than a general organellar perturbation conditions the *msh1* changes.

The hemicomplementation assay was designed to not only discriminate between the mitochondrial and plastid contributions to the derived phenotype but to assess whether MSH1 might also function within the nucleus. No nuclear localization is evident in MSH1-GFP reporter transgene experiments with laser scanning confocal microscopy (Xu et al., 2011). Still, the

Table IV. *Sample Arabidopsis gene expression changes observed in association with altered phenotypes (genes, shown as fold change, significant at a false discovery rate of less than 0.1)*

Boldface designates down-regulation, roman designates up-regulation.

Arabidopsis Genome Initiative No.	Gene	*msh1*
Cell cycle and growth		
AT1G76540	CDKB2;1	−1.7
AT2G26760	CYCB1;4	−1.3
AT4G34160	CYCD3	−1.8
AT2G44740	CYCP4;1	−1.7
AT2G40610	EXPA8	−1.4
AT1G20190	EXPA11	−2.6
Redox/oxidative stress responsive		
AT3G22370	AOX1A	2.2
AT3G30775	ERD5	2.3
AT5G20230	ATBCB	10.9
AT5G62520	SRO5	3.7
AT2G21640	Oxidative stress response	2.9
AT4G20830	FAD-binding domain protein	2.6
AT3G29250	Oxidoreductase	2.1
GA related		
AT1G02400	ATGA20X6	4.4
AT1G75750	GASA1	2.7
AT1G74670	GASA6	−1.5
AT2G14900	GA-regulated protein	−4.5
Auxin related		
AT4G39950	CYP79B2	−2.4
AT2G22330	CYP79B3	−2.3
AT1G73590	PIN1	−1.5
AT1G23080	PIN7	−1.6
AT3G23050	IAA7	−1.6

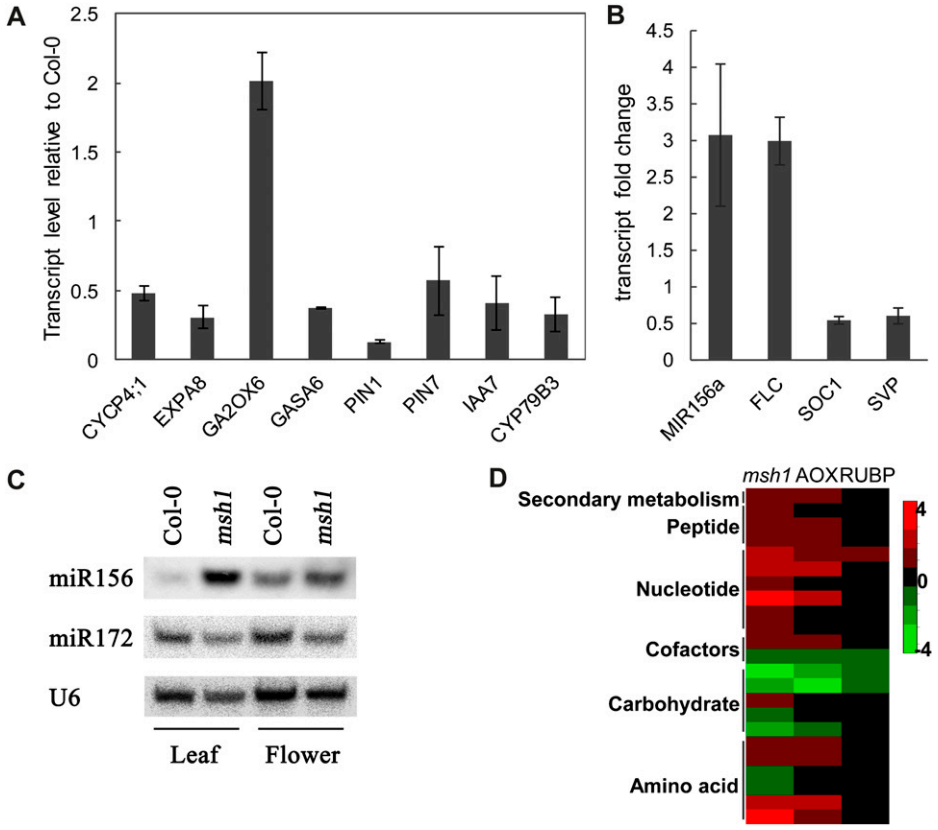

Figure 5. Evidence of transcriptional and metabolic changes in Arabidopsis *msh1* mutant and hemicomplementation lines. A, Results from quantitative RT-PCR analysis of the *msh1* mutant showing transcript-level changes in several genes controlling growth (cyclin P4:1 and Expansin), GA_3 (Gibberellin2 Oxidase6 and GA-STIMULATED ARABIDOPSIS6), and auxin levels (PIN1/PIN7 AUXIN EFFLUX CARRIERS, IAA7 AUXIN-RESPONSIVE PROTEIN, and CYTOCHROME P450 79B3) in the plant. B, Quantitative RT-PCR assay of transcript levels from the four flowering-related genes *MIR156*, *FLC*, *SOC1*), and *SHORT VEGETATIVE PHASE* (*SVP*) in Col-0 and *msh1* plants. Data are shown as fold change relative to the wild type (Col-0) with means ± SE from three biological replicates. C, RNA gel blot assay of rosette leaf and flower tissues for the flowering-related microRNAs *miR156* and *miR172*. U6 was used as a loading control. D, A heat map with a subset of metabolites assayed in the study, comparing relative accumulation patterns in *msh1*, the mitochondrial hemicomplementation line (AOX), and the plastid hemicomplementation line (RUBP).

transgenerational heritability of observed phenotypic changes implies epigenetic influences on nuclear gene expression. Our ability to fully complement the altered growth phenotype with a plastid-targeted MSH1 transgene, but not with a mitochondria-targeted transgene, argues against the nuclear localization of MSH1. Rather, our data suggest that changes in plastid state affect the phenotypic changes that are subsequently heritable, implying that these plastid changes condition an epigenetic effect.

The components of transgenerational phenotypic plasticity in plants are maternal (Galloway and Etterson, 2007; Donohue, 2009), and several of these appear to be adaptive under particular environments. However, there has been little or no direct evidence of organellar changes underlying these processes. Suppression of *MSH1* expression produces cytoplasmic male sterility and variegation through direct DNA rearrangement of the chloroplast and mitochondrial genomes, but the additional phenotypic plasticity described in this study appears to derive from plastidial signaling. Heritable and cross-species reproducibility of the phenotypic changes, co-opting well-defined, nucleus-controlled developmental pathways, and the complete reversal of phenotype with pollination by wild-type plants suggest epigenetic processes. Epigenomic changes appear to underlie at least some of the environmentally responsive phenotypic plasticity observed in natural systems (Bonduriansky and Day, 2009). In fact, *MSH1* transcript levels show environmental responsiveness, with dramatically reduced levels under conditions of stress (Hruz et al., 2008; Shedge et al., 2010; Xu et al., 2011). Moreover, disruption of *MSH1* produces an altered redox state of the plastid (Xu et al., 2011), implying one means of signaling cellular change. We suggest that *MSH1* modulation operates in plants, under natural conditions, to link mechanisms for environmental sensing with genomic responses by triggering organellar mediators of the process.

Table V. *Metabolite changes in Arabidopsis msh1 and sorghum MSH1-RNAi plants*

N.D., The metabolite was nondetectable.

Pathway	Metabolite	Arabidopsis[a]	Sorghum[a]
Stress response			
Ascorbate metabolism	Ascorbate	1.89	1.59
Tocopherol metabolism	α-Tocopherol	1.79	2.42
Amino sugar and nucleotide sugar	Erythronate	1.48	1.99
	Ribitol		3.58
	Ribulose		5.79
Suc, Glc, and Fru metabolism	Maltose	1.39	1.9
	Mannitol	9.46	3.12
Ser family	Betaine	3.14	1.92
Phenylpropanoids	Sinapate	7.31	–[b]
Amines and polyamines	Putrescine	5.03	
	Spermidine	2.21	
Arg metabolism	1,3-Diaminopropane	6.41	
	Arg	5.08	
	Citrulline	1.67	
Glutathione metabolism	Glutathione (oxidized)	1.50	
Flavonoid	Apigenin	–	9.40
	Apigenin-7-*O*-glucoside	–	6.81
	Isovitexin	–	2.34
	Kaempferol-3-*O*-β-glucoside	–	2.23
	Luteolin-7-*O*-glucoside	–	6.67
	Vitexin		2.46
Energy metabolism			
Suc, Glc, and Fru metabolism	Suc	N.D.	0.64
	Raffinose	N.D.	0.74
Protein turnover			
Dipeptide	Ala	1.67	
	Alanyl-Ile	1.95	
	Alanyl-Leu	2.16	
	Alanyl-Phe	1.76	
	Glycyltyrosine	1.80	
	Isoleucyl-Leu	1.69	
	Leucyl-Leu	2.14	
Nucleic acid turnover			
Purine metabolism	Adenosine-2′,3′-cyclic monophosphate	2.56	
	Guanosine-2′,3′-cyclic monophosphate	3.08	

[a]Fold change in metabolite level in *msh1* relative to the wild type in Arabidopsis and sorghum with significance at $P \leq 0.05$. [b]The metabolite was not present in the species.

We observe coinheritance of variation in flowering time, plant growth rate, branching patterns, stomatal density changes, and maturity transition in Arabidopsis and sorghum. Phenotypic variation for these quantitative traits has been the subject of ecological association mapping studies to understand genotype-by-environment interactions and plant adaptation in natural environments (Bergelson and Roux, 2010). Our results suggest that epigenetic, or "soft," inheritance processes may support a coordinated modulation of all of these traits in response to environmental cues.

MATERIALS AND METHODS

Plant Materials and Growth Conditions

Arabidopsis (*Arabidopsis thaliana*) ecotype Columbia (Col-0) and *msh1* mutant lines were obtained from the Arabidopsis stock center and grown in Metro Mix at 24°C. The development of RNAi suppression lines of tomato (*Solanum lycopersicum*) and tobacco (*Nicotiana tabacum*; Sandhu et al., 2007), millet (*Pennisetum americanum*) and sorghum (*Sorghum bicolor*; Xu et al., 2011), and Arabidopsis hemicomplementation lines (Xu et al., 2011) is described elsewhere. Individual RNAi constructs were developed to target the same region of MSH1 domain VI in each species, and analysis of phenotypes is based on five lead events carried forward of tomato and tobacco, three of millet, and one of sorghum. Tx430 is an inbred sorghum line (Miller, 1984) maintained in the University of Nebraska, Lincoln, sorghum breeding program and used for the development of the *MSH1*-RNAi transgenic line. Arabidopsis flowering time was measured as the date of first visible flower bud appearance. At this time, total rosette leaf number was also determined as flowering rosette leaf number.

For GA treatment, 3-week-old Arabidopsis plants were treated with 100 μM GA_3 twice a week for 3 weeks. Sorghum plants were treated twice with 2,500 ppm GA_3 starting prior to the transition to reproduction, with treatments 2 weeks apart.

For studies of metabolism and transcript levels, Arabidopsis plant staging was carried out based on leaf number, and plants of the same age were used for all experiments. The *msh1* mutants are considerably smaller than wild-type plants at the same age, determined as days after germination. Plant sampling stage was just before bolting. For sorghum analysis, plants were taken at the five- to six-leaf stage. All plants were grown under controlled growth room conditions.

Figure 6. Hemicomplementation analysis of the Arabidopsis *msh1* altered growth phenotype. The wild type (Col-0), the *msh1* mutant, and dual-targeted, plastid-targeted, and mitochondria-targeted *MSH1* transgenic complementation lines were grown under 10-h photoperiod conditions. Approximately 60 plants were grown for each line, and flowering time was recorded for each individual plant. Shown are sample plants at 14 weeks. Col-0, dual-targeted, and plastid-targeted *MSH1* transgenic lines flowered uniformly, whereas the *msh1* mutant and the mitochondria-targeted *MSH1* transgenic line showed marked variation for growth, flowering time, and maturity.

Microscopy

The autofluorescence images of secondary growth were produced with fresh, hand-sectioned Arabidopsis stems on a Nikon A1 laser scanning confocal microscope. Excitation lines and emission filters were 405, 488, 561, and 641 nm and 425 to 475, 500 to 550, 570 to 620, and 662 to 737 nm. For light microscopic analyses, stems were fixed with 4% formaldehyde in 50 mM phosphate buffer, pH 7.0, under vacuum for 1 h. Samples were dehydrated in a graduated ethanol series, embedded in LR White (Electron Microscopic Sciences), and sectioned (500 nm) for staining with 1% toluidine blue light microscopy (Olympus Provis). Samples for stomatal density were prepared from adaxial and abaxial surfaces of the middle section of mature sorghum leaves. Samples were observed with a Nikon Eclipse E800 light microscope (20×) with image area captured at 0.307 mm^2. Stomata number was estimated with NIH ImageJ software and analyzed with the GLIMMIX procedure (SAS 9.2).

RNA Isolation and Real-Time PCR Analysis

Total Arabidopsis and sorghum RNA was extracted from aboveground tissues of wild-type and mutant or RNAi plants using the TRIzol (Invitrogen) extraction procedure followed by purification on RNeasy columns (Qiagen). cDNA was synthesized with SuperScriptIII first-strand synthesis SuperMix for quantitative RT-PCR (Invitrogen). Quantitative PCR was performed on the iCycler iQ system (Bio-Rad) with SYBR GreenER Supermix (Invitrogen). PCR primers are listed in Supplemental Table S3. For sorghum assays, primers were designed to the 3′ region of *MSH1*. The transcript level of each gene was normalized to UBIQUITIN10.

RT-PCR analysis also involved multiple plant stages, ranging from 2 weeks old to flowering stage, to confirm the results observed by global transcriptome analysis.

Small RNA Analysis

RNA isolation and microRNA hybridization were performed as described by others (Park et al., 2002). Total RNA was exacted with TRIzol, and small-sized RNA was enriched by treatment with 5% PRG8000 in 0.5 M NaCl and then precipitated with ethanol and glycogen. RNA was resolved on 16% denaturing acrylamide gels, and small RNA was detected by ^{32}P end-labeled specific RNA/DNA probes.

Genomic DNA Methylation Assay

Genomic DNA (approximately 500 ng) was used for bisulfite treatment using the EpiTect Bisulfite kit (Qiagen). Each sample was sodium bisulfite treated twice and subjected to a first round of PCR amplification with primers 3-2R and 3-2L (Supplemental Table S4). The PCR product was reamplified with nested primers 3-2Ln and 3-2R. Conditions used were 46°C for 30 cycles and Accuprime-Taq DNA polymerase kit (Invitrogen). The amplified products of 250 bp were eluted, sequenced, and aligned against an untreated genomic DNA sequence with T-COFFEE. At least two independent bisulfite treatments and two independent PCR products per bisulfite treatment were prepared for each sample (four runs total per line), followed by sequence analysis.

Metabolite Analysis

Metabolic profiling analysis of all samples was carried out in collaboration with Metabolon according to the methods described previously (Oliver et al., 2011). The global unbiased metabolic profiling platform involved a combination of three independent platforms: ultra-HPLC (UHPLC)-tandem mass spectrometry (MS/MS) optimized for basic species, UHPLC/MS/MS optimized for acidic species, and gas chromatography-MS. Samples in six replicates were extracted, analyzed with the three instruments, and their ion features were matched against a chemical library for identification. For sample extraction, 20 mg of each leaf sample was thawed on ice and extracted using an automated MicroLab STAR system (Hamilton Co.) in 400 μL of methanol

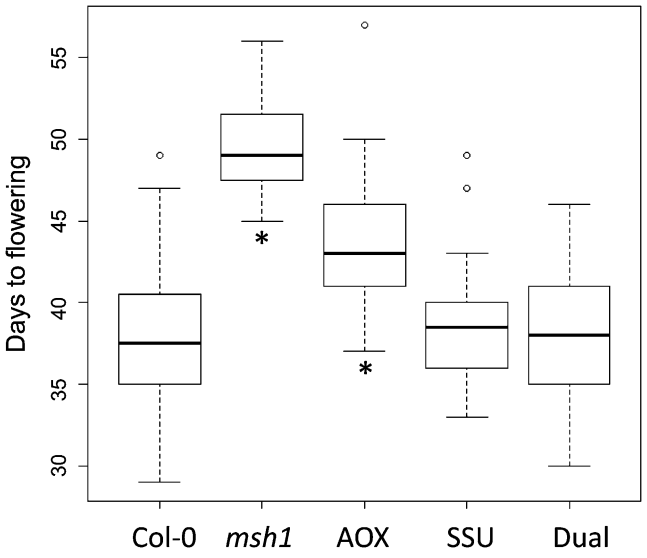

Figure 7. Days to flowering in Arabidopsis Col-0, *msh1*, and hemicomplementation lines grown in a 12-h photoperiod. Col-0, SSU (plastid-targeted MSH1), and Dual (dual-targeted MSH1) flower uniformly, whereas *msh1* and AOX (mitochondria-targeted MSH1) flower significantly later ($P < 0.001$). The *msh1* plants were randomly selected.

containing recovery standards. UHPLC/mass spectrometry (MS) was performed using a Waters Acquity UHPLC device coupled to an LTQ mass spectrometer (Thermo Fisher Scientific) equipped with an electrospray ionization source. Two separate UHPLC/MS injections were performed on each sample: one optimized for positive ions and one for negative ions. Derivatized samples for gas chromatography-MS were analyzed on a Thermo-Finnigan Trace DSQ fast-scanning single-quadrupole mass spectrometer operated at unit mass resolving power. Chromatographic separation, followed by full-scan mass spectra, was performed to record retention time, mass-to-charge ratio, and MS/MS of all detectable ions present in the samples. Metabolites were identified by automated comparison of the ion features in the experimental samples with a reference library of chemical standard entries that included retention time, mass-to-charge ratio, preferred adducts, and in-source fragments as well as their associated MS/MS spectra.

For hormone metabolic profiling, 4-week-old Arabidopsis and 2-week-old sorghum seedlings were collected, frozen, and lyophilized. Profiling was conducted at the National Research Council Plant Biotechnology Institute in Saskatoon, Canada, according to Chiwocha et al. (2005).

Microarray Experiments

Microarray experiments were carried out as described by Xu et al. (2011). Total RNA was extracted from 8-week-old Col-0 and *msh1* mutant Arabidopsis plants using TRIzol (Invitrogen) extraction procedures followed by purification on RNeasy columns (Qiagen). Three hybridizations were performed per genotype with RNA extractions from single plants for each microarray chip. Samples were assayed on the Affymetrix GeneChip oligonucleotide 22K ATH1 array (Affymetrix) according to the manufacturer's instructions. Expression data from Affymetrix GeneChips were normalized using the robust multichip average method (Bolstad et al., 2003). A separate mixed linear model analysis was conducted using the normalized data with SAS software (Wolfinger et al., 2001). Each mixed model includes a fixed effect for genotype and a random effect for experiment. Tests for differential expression across genotypes were performed as part of our mixed linear model analyses. The P values generated from tests of interest were converted to q values to obtain approximate control of the false discovery rate at a specified value (Storey and Tibshirani, 2003). We obtained estimates of fold change for each probe by converting the mean treatment difference estimated as part of our mixed linear model analyses.

The microarray data have been deposited at the Gene Expression Omnibus (GSE35893). Sequence data from this article can be found in the GenBank/EMBL data libraries under the accession numbers listed in Table IV.

Supplemental Data

The following materials are available in the online version of this article.

Supplemental Figure S1. Measurement of growth parameters for sorghum MSH1-RNAi.

Supplemental Figure S2. PCR products derived from sorghum T3.

Supplemental Figure S3. Additional MSH1 methylation analysis.

Supplemental Table S1. Frequency of msh1-dr plants in T3.

Supplemental Table S2. Stomatal number in sorghum.

Supplemental Table S3. Plant height measurements.

Supplemental Table S4. Primers used.

ACKNOWLEDGMENTS

We thank Natalya Nersesian and Shirley Sato and the University of Nebraska, Lincoln, Center for Biotechnology Plant Transformation Core Facility for technical assistance with developing transformed plant materials: Hardik Kundariya for technical assistance, Christian Elowsky and Han Chen for microscopy of Arabidopsis, and Tom Elthon for technical assistance with phenotype assays.

Received February 20, 2012; accepted April 6, 2012; published April 9, 2012.

LITERATURE CITED

Abdelnoor RV, Christensen AC, Mohammed S, Munoz-Castillo B, Moriyama H, Mackenzie SA (2006) Mitochondrial genome dynamics in plants and animals: convergent gene fusions of a MutS homologue. J Mol Evol **63:** 165–173

Abdelnoor RV, Yule R, Elo A, Christensen AC, Meyer-Gauen G, Mackenzie SA (2003) Substoichiometric shifting in the plant mitochondrial genome is influenced by a gene homologous to *MutS*. Proc Natl Acad Sci USA **100:** 5968–5973

Arrieta-Montiel MP, Shedge V, Davila J, Christensen AC, Mackenzie SA (2009) Diversity of the Arabidopsis mitochondrial genome occurs via nuclear-controlled recombination activity. Genetics **183:** 1261–1268

Bergelson J, Roux F (2010) Towards identifying genes underlying ecologically relevant traits in *Arabidopsis thaliana*. Nat Rev Genet **11:** 867–879

Bolstad BM, Irizarry RA, Astrand M, Speed TP (2003) A comparison of normalization methods for high density oligonucleotide array data based on variance and bias. Bioinformatics **19:** 185–193

Bonduriansky R, Day T (2009) Nongenetic inheritance and its evolutionary implications. Annu Rev Ecol Evol Syst **40:** 103–125

Chiwocha SD, Cutler AJ, Abrams SR, Ambrose SJ, Yang J, Ross AR, Kermode AR (2005) The *etr1-2* mutation in *Arabidopsis thaliana* affects the abscisic acid, auxin, cytokinin and gibberellin metabolic pathways during maintenance of seed dormancy, moist-chilling and germination. Plant J **42:** 35–48

Danchin É, Charmantier A, Champagne FA, Mesoudi A, Pujol B, Blanchet S (2011) Beyond DNA: integrating inclusive inheritance into an extended theory of evolution. Nat Rev Genet **12:** 475–486

Davila JI, Arrieta-Montiel MP, Wamboldt Y, Cao J, Hagmann J, Shedge V, Xu YZ, Weigel D, Mackenzie SA (2011) Double-strand break repair processes drive evolution of the mitochondrial genome in Arabidopsis. BMC Biol **9:** 64

Donohue K (2009) Completing the cycle: maternal effects as the missing link in plant life histories. Philos Trans R Soc Lond B Biol Sci **364:** 1059–1074

Fornara F, de Montaigu A, Coupland G (2010) SnapShot: control of flowering in Arabidopsis. Cell **141:** 550, 550, e1–e2

Galloway LF (2005) Maternal effects provide phenotypic adaptation to local environmental conditions. New Phytol **166:** 93–99

Galloway LF, Etterson JR (2007) Transgenerational plasticity is adaptive in the wild. Science **318:** 1134–1136

Gill SS, Tuteja N (2010) Polyamines and abiotic stress tolerance in plants. Plant Signal Behav **5:** 26–33

Hruz T, Laule O, Szabo G, Wessendorp F, Bleuler S, Oertle L, Widmayer P, Gruissem W, Zimmermann P (2008) Genevestigator v3: a reference expression database for the meta-analysis of transcriptomes. Adv Bioinformatics **2008:** 420747

Ingram J, Bartels D (1996) The molecular basis of dehydration tolerance in plants. Annu Rev Plant Physiol Plant Mol Biol **47:** 377–403

Johannes F, Colot V, Jansen RC (2008) Epigenome dynamics: a quantitative genetics perspective. Nat Rev Genet **9:** 883–890

Miller FR (1984) Registration of RTx430 sorghum parental line. Crop Sci **24:** 1224

Nakano T, Nagata N, Kimuro T, Sekimoto M, Kawaide H, Murakami S, Kaneko Y, Matsuchima H, Kamiya Y, Sato F, et al (2003) CND41, a chloroplast nucleoid protein that regulates plastid development, causes reduced gibberellin content and dwarfism in tobacco. Physiol Plant **117:** 130–136

Ogata H, Ray J, Toyoda K, Sandaa RA, Nagasaki K, Bratbak G, Claverie JM (2011) Two new subfamilies of DNA mismatch repair proteins (MutS) specifically abundant in the marine environment. ISME J **5:** 1143–1151

Oliver MJ, Guo L, Alexander DC, Ryals JA, Wone BW, Cushman JC (2011) A sister group contrast using untargeted global metabolomic analysis delineates the biochemical regulation underlying desiccation tolerance in *Sporobolus stapfianus*. Plant Cell **23:** 1231–1248

Park W, Li J, Song R, Messing J, Chen X (2002) CARPEL FACTORY, a Dicer homolog, and HEN1, a novel protein, act in microRNA metabolism in *Arabidopsis thaliana*. Curr Biol **12:** 1484–1495

Sakamoto W (2003) Leaf-variegated mutations and their responsible genes in *Arabidopsis thaliana*. Genes Genet Syst **78:** 1–9

Sandhu AP, Abdelnoor RV, Mackenzie SA (2007) Transgenic induction of mitochondrial rearrangements for cytoplasmic male sterility in crop plants. Proc Natl Acad Sci USA **104:** 1766–1770

Sangster TA, Queitsch C (2005) The HSP90 chaperone complex, an emerging force in plant development and phenotypic plasticity. Curr Opin Plant Biol **8:** 86–92

Shedge V, Arrieta-Montiel M, Christensen AC, Mackenzie SA (2007) Plant mitochondrial recombination surveillance requires unusual RecA and MutS homologs. Plant Cell **19:** 1251–1264

Shedge V, Davila J, Arrieta-Montiel M, Mohammed S, Mackenzie SA (2010) Extensive rearrangement of the Arabidopsis mitochondrial genome elicits cellular conditions for thermotolerance. Plant Physiol **152:** 1960–1970

Storey JD, Tibshirani R (2003) Statistical significance for genomewide studies. Proc Natl Acad Sci USA **100:** 9440–9445

Willige BC, Isono E, Richter R, Zourelidou M, Schwechheimer C (2011) Gibberellin regulates PIN-FORMED abundance and is required for auxin transport-dependent growth and development in *Arabidopsis thaliana*. Plant Cell **23:** 2184–2195

Wolfinger RD, Gibson G, Wolfinger ED, Bennett L, Hamadeh H, Bushel P, Afshari C, Paules RS (2001) Assessing gene significance from cDNA microarray expression data via mixed models. J Comput Biol **8:** 625–637

Xu YZ, Arrieta-Montiel MP, Virdi KS, de Paula WB, Widhalm JR, Basset GJ, Davila JI, Elthon TE, Elowsky CG, Sato SJ, et al (2011) MutS HOMOLOG1 is a nucleoid protein that alters mitochondrial and plastid properties and plant response to high light. Plant Cell **23:** 3428–3441

Yu F, Fu A, Aluru M, Park S, Xu Y, Liu H, Liu X, Foudree A, Nambogga M, Rodermel S (2007) Variegation mutants and mechanisms of chloroplast biogenesis. Plant Cell Environ **30:** 350–365

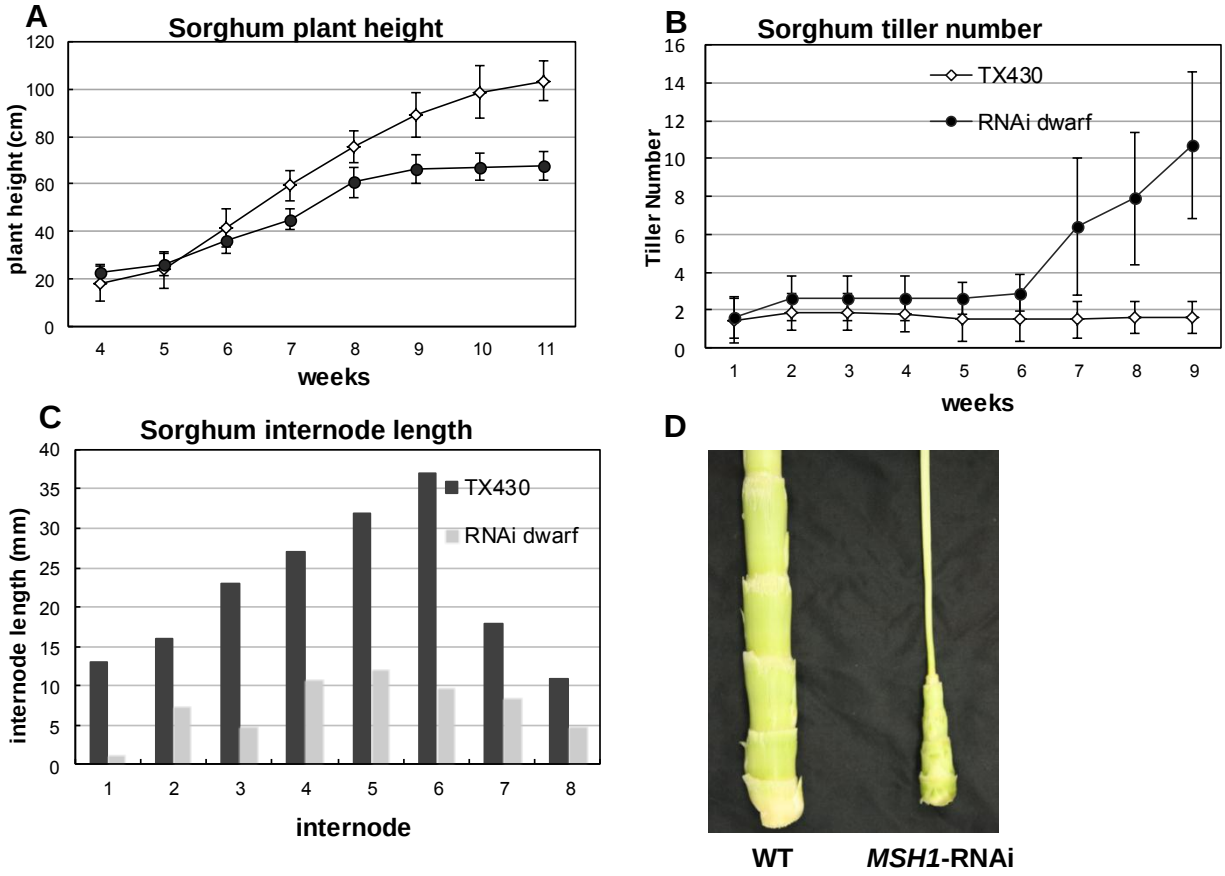

Supplementary Figure 1. Measurement of growth parameters for the sorghum *MSH1*-RNAi variant phenotype. Plant height (A) and tiller number (B) was measured over time for three wildtype Tx430 and three dwarfed *MSH1*-RNAi sorghum plants. (C) Internode length measurements were averaged from three plants per genotype, with the marked differences shown in (D).

Supplementary Figure 2. PCR products derived from T3 sorghum plants displaying the MSH1-dr phenotype. Primers used (Supplementary Table 3) were designed to amplify a 750-bp segment of the RNAi transgene. Lane 10 shows results from wildtype Tx430.

1. MW Marker **6. GAII24** **11. -template**
2.GAII11 **7. GAII25** **12. 7.8**
3.GAII15 **8. GAII28** **13. 8.6**
4.GAII22 **9. GAII32** **14. 9.1**
5.GAI14 **10.TX430 WT**

Supplementary Figure 2. PCR-based assay to confirm presence/absence of MSH1-RNAi transgene in sorghum plants. The predicted product is 750 bp. Lane 10 contains negative control sample from wildtype Tx430 and lane 11 contains a negative control reaction prepared minus template. Primers used for the assay are listed in Supplementary Table 4.

Supplementary Figure 3. Additional *MSH1* methylation analysis. DNA samples from five T4 sorghum lines containing the MSH1-RNAi transgene (2-9, 7-8, 8-6, 9-17 and 9-16) and four lines lacking the transgene but displaying the MSH1-dr phenotype (GAII-25, -11, -22 and -28) were bisulfite treated, together with Tx430 wildtype (WT treated) and DNA sequenced for the interval of the *MSH1* gene targeted by the RNAi transgene. Red boxes designated three sites showing differential methylation. In all cases, the lines lacking the transgene appear to resemble the wildtype line. WT designates Tx430 DNA sequence from sample that was not bisulfite-treated. Each sample was sequenced four times, with one representative sample shown.